SPE-185557-MS

New Methodology for Pore Pressure Prediction Using Well Logs and Divergent Area

D. Velázquez-Cruz, G. Espinosa-Castañeda, M. A. Díaz-Viera, and F. Leyte-Guerrero, Instituto Mexicano Del Petróleo

This paper was prepared for presentation at the SPE Latin America and Caribbean Petroleum Engineering Conference held in Buenos Aires, Argentina, 18-19 May 2017.

Abstract

The pore pressure prediction is the most important process in the design of drilling wells. This paper depicts a new methodology to analyze pore pressure based on both, the normal compaction theory of sediments and the way that normal behavior diverges when it is interrupted. Much has been written on the topic; however, even today a high percentage of non-productive time (NPT) in drilling activities is related to pore pressure and wellbore instability problems. Here, a new methodology is proposed to improve the accuracy of calculated pore pressure from well logs and seismic data. Moreover, this new methodology allows, under specific conditions, to determine pore pressure in carbonates and other reservoir rocks. The compaction process defines the normal trend of porosity indicators with depth, the fluid retention depth and those rock bodies diverging from a normal compaction trend. The divergence detection procedure includes the identification of both, transitional changes of the porosity indicators (shale) and those that are parallel to normal compaction trend (reservoir rock); they allow to build a divergent area. When the divergent area is defined, the pore pressure calculation can be done using a pore pressure model based on normal compaction theory and well logs or interval velocity data from seismic. Misleading prediction of geopressures for a particular area are linked to: misunderstandings of pore pressure origins there, the limited scope of pore pressure models based on well logs and to miscalculations of the key parameters of pore pressure models. This work discuss the impact of these key parameters in the pore pressure prognosis. Analysis of actual cases showing the impact of miscalculation of overburden stress on pore pressure estimations, normal compaction trend definition and pore pressure calculations are presented using divergent area along with the Eaton model. The conclusions support the following statements: well log density data cannot be used to calculate the overburden pressure and under some conditions, the divergence methodology can be used to calculate pore pressures in carbonates. Furthermore, the divergent area method eliminate the use of shale points in pore pressure prognosis.

Introduction

The analysis of abnormal pressures is an issue that has been studied for more than 50 years, however, even today a high percentage of non-productive time (NPT) in drilling activities is related to pore pressure and wellbore instability problems (Hamid et al. 2016; Ong et al. 2015; York et al. 2009). The misleading prediction of geopressures are linked to misunderstandings of the pore pressure genesis for a particular area and to the limited scope of pore pressure models based on well logs and miscalculations of the key parameters of pore pressure models.

Swarbrick and Osborne (1998) describe several mechanisms that originates abnormal pressures, which must be taken into account for pore pressure prognosis during drilling well design. Furthermore, despite the broad causes of abnormal pressures in the earth's crust, the mathematical prediction models that use either well logs or seismic data only predict pore pressure generated by stress-related mechanisms; this is also know as "*compaction disequilibrium*" or "*undercompaction*". Figure 1 shows a pressure-depth plot illustrating the existence of other pore pressure mechanisms, which must be taken into account to improve pressure predictions.

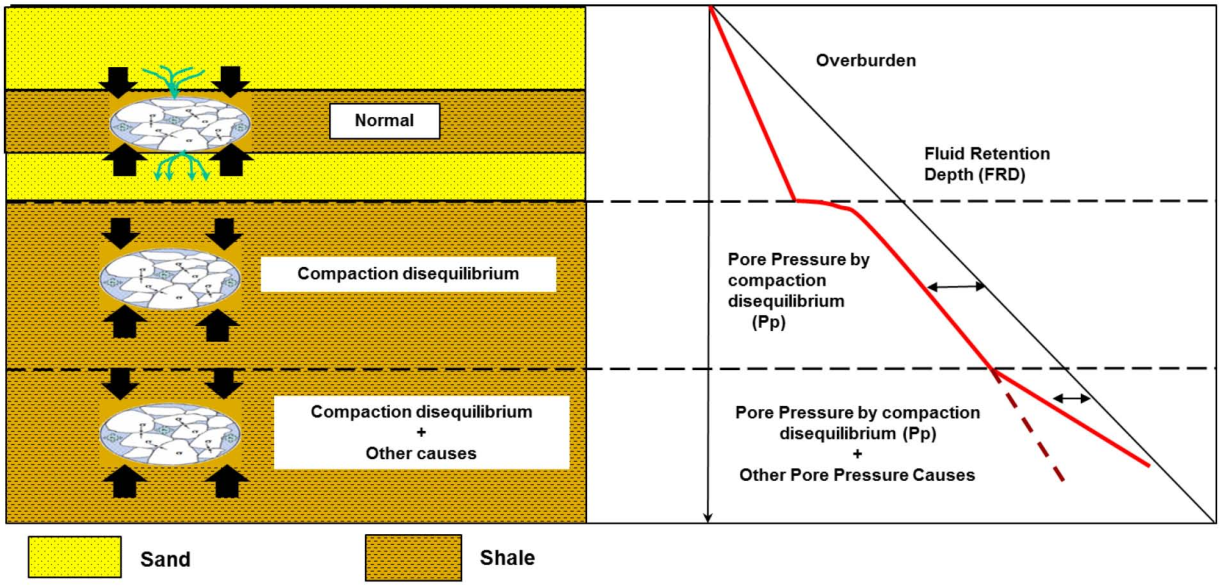

Figure 1—Pore pressure is because of combination of several mechanisms (Modified from Bowers 2002).

Hence, because shales are more sensitive to undercompaction phenomena, the prognosis of abnormal pressures focuses on their behavior (Hottmann, and Johnson 1965; Bowers 2002). However, when we have reservoir type rocks (sands or carbonates), the prognosis of pore pressure using well logs or seismic data do not match altogether with recorded pore pressures (Green et al. 2016; Hoskin and O'Connor 2016). Figure 2 describes pore pressure prognosis behavior in a shale and reservoir type rock (sands). The black dots are pore pressure values measured in a reservoir type rock; the continuous line represent the predicted pore pressure values determined from well logs. This behavior is because the reservoir rock do not follows overall the compaction theory such as shales (Terzaghi and Peck 1938; Hottmann and Johnson 1965) and/or the generation of reservoir pore pressure is due to other pressure mechanism different to undercompaction.

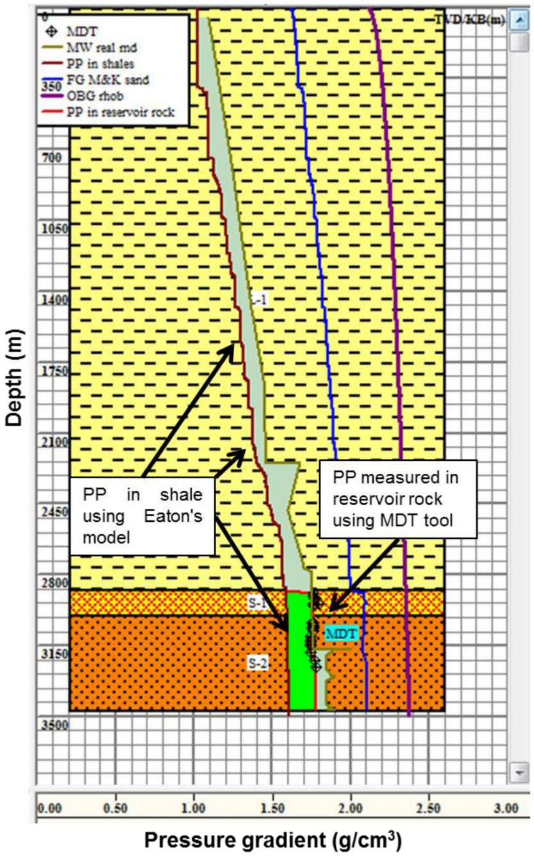

Figure 2—Behavior of pore pressure in shale and reservoir rock.

The most commonly used pore pressure models in industry are based on the theory of normal sediment compaction described by Terzaghi and Peck (1948). Here the pore pressure models consider the behavior of porosity (or porosity indicators such as sonic transit time, resistivity or interval velocity) with depth to define the compaction disequilibrium; this behavior is called normal compaction trend (NCT). Shaker (2007a, 2007b) discussed the importance of NCT in pore pressure prediction and show examples of NCT data manipulation for calibration purposes. Figure 3 shows the NCT plotted correctly against a NCT plotted in several segments with the purpose of fitting pore pressure measured values.

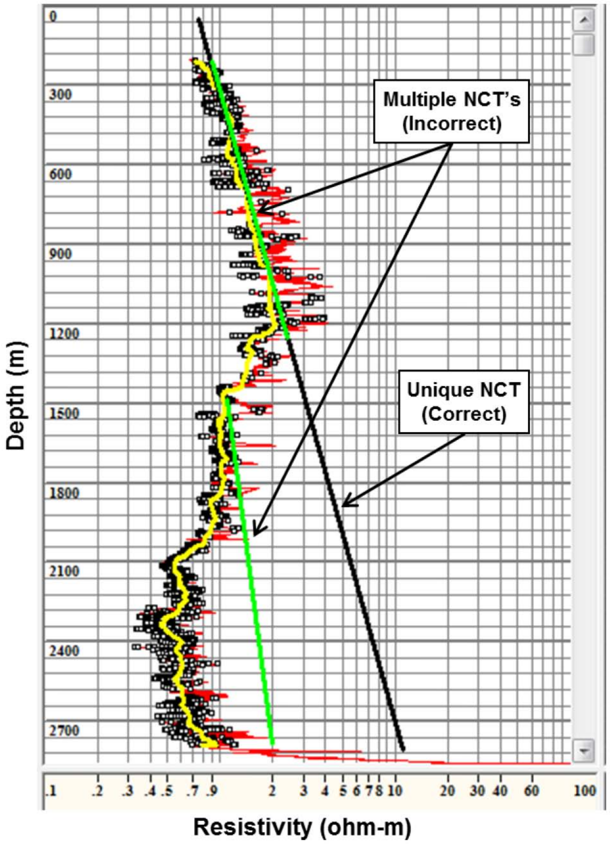

Figure 3—Unique NCT and multiple NCT for fitting purposes.

In addition, the models have parameters that have to be adjusted depending on the geological frame of each particular basin. For example, Lopez-Solis and Velazquez-Cruz (2006) discuss an study of normal compaction trends for resistivity in Mexican offshore wells and put forward the adjustments to Eaton's model for correct pore pressure prediction in Mexican Gulf Coast.

This work discuss the impact of these key parameters in the pore pressure prognosis. Analysis of real cases that show the impact of miscalculation of overburden stress and normal compaction trend definition are presented as well as pore pressure calculations using divergent area and Eaton's model.

Strategy for Pore Pressure Analysis

A systemic approach called "*convergence analysis*" was followed in this paper, which includes: the definition of Normal Compaction Trend (NCT), the determination of Fluid Retention Depth (FRD), setting up of divergent area, an overburden correction by effect of density log and the fitting of a pore pressure model. Figure 4 schematizes the different elements integrated in the convergence analysis.

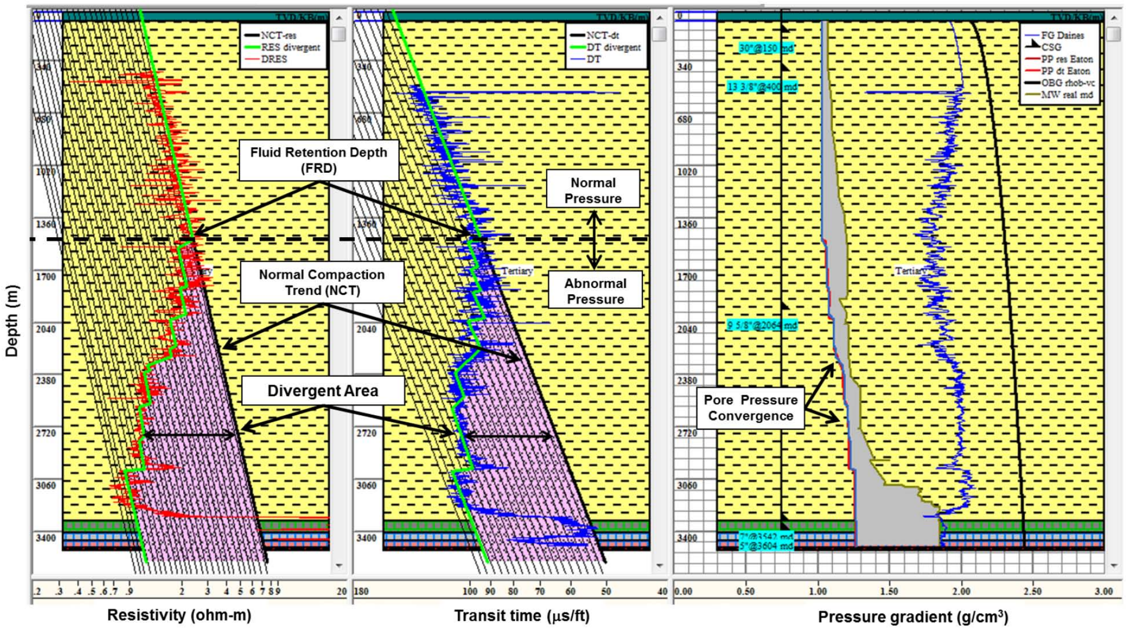

Figure 4—Approach of convergence for pore pressure analysis.

Analysis of Normal Compaction Trend (NCT)

Pore pressure models based on effective stress consider the definition of a NCT against depth. The NCT represents the loss of porosity because of compaction when sediments burial increase. Hottmann and Johnson (1965) showed that when the porosity reduces with depth, the pressure in porous media is normal. Conversely, when the porosity is anomalously high for burial depth the pore pressure is abnormally high. Therefore, if the loss of porosity against depth behaves as an exponential function (Athy 1930), the NCT can be represented as:

$$\phi_n = \phi_o e^{-c \cdot Z} \tag{1}$$

Where:

ϕ_n = Normal compaction trend for porosity

ϕ_o = Porosity at surface

c = Normal compaction behavior index

Z = Depth

Generalizing equation (1) for other indicators of porosity loss with depth such as sonic transit time, interval velocity and resistivity; they are portrayed as:

$$\Delta t_n = \Delta t_o e^{-c \cdot Z} \tag{2}$$

$$V_n = V_o e^{c \cdot Z} \tag{3}$$

$$R_n = R_o e^{c \cdot Z} \tag{4}$$

Where:

Δt_n = Normal compaction trend for sonic transit time

Δt_o = Sonic transit time at surface

V_n = Normal compaction trend for interval velocity

V_o = Interval velocity at surface

R_n = Normal compaction trend for resistivity

R_o = Resistivity at surface

c = Normal compaction behavior index
Z = Depth

Figure 5 describes the behavior of NCT with depth; when loss of porosity progress with depth because of geostatic compaction, it behaves like an exponential function (dashed line); when compaction is interrupted, the porosity "diverges" from its normal compaction trend (dotted line in red zone). If the NCT represents the porosity loss with depth, then any well would have a unique NCT as shown in figure 5 (dashed line). As pointed out by Shaker (2007a), the NCT is the keystone of pore pressure analysis and breaking the NCT into several segments for calibration purposes must be avoided (figure 6).

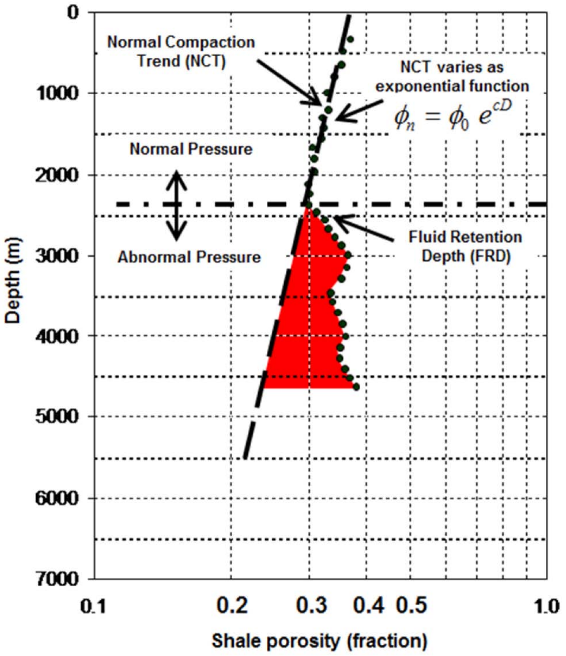

Figure 5—Behavior of porosity with depth.

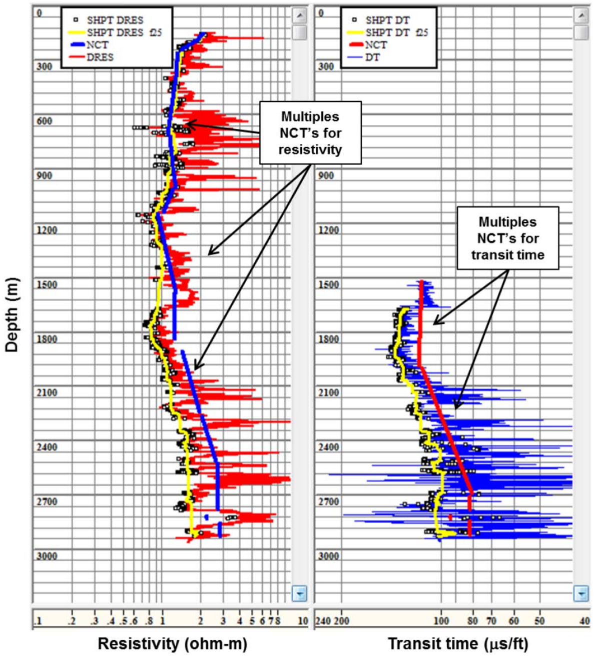

Figure 6—Breaking NCT in multiple trends for calibration purposes of pore pressure

The analysis of behavior of NCT must be both, systematic and in concordance with rock compaction increase in any particular basin. Pennebaker (1968) and Correa (2016) discuss how the NCT behaves when related to interval velocity, sonic transit time and resistivity for the Gulf Basin and Burgos Basin (figure 7).

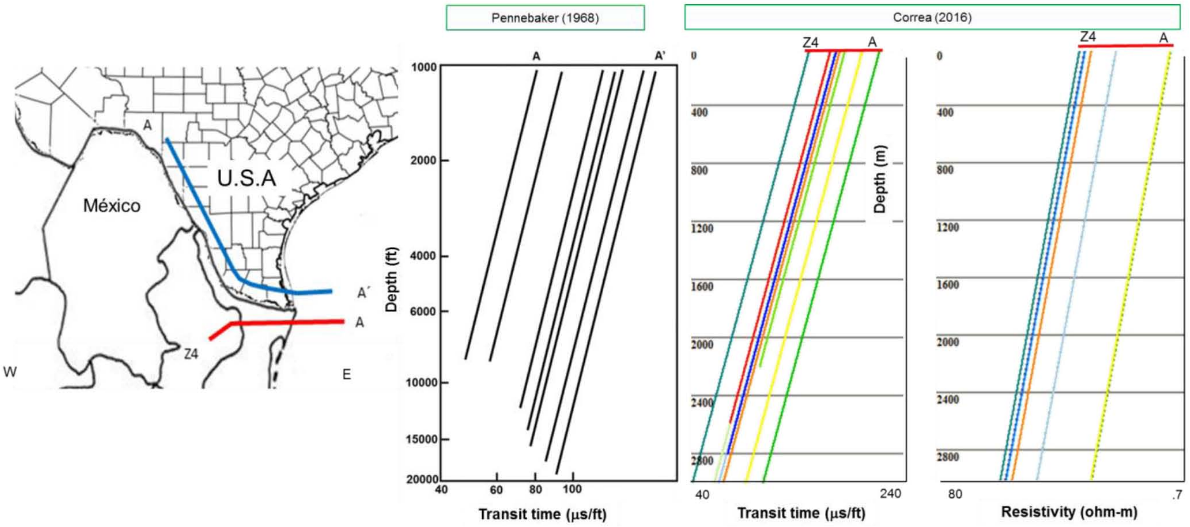

Figure 7—Behavior of NCT for different porosity indicators and basins.

Fluid Retention Depth (FRD)

As burial depth increase, porosity reduces until a depth known as Fluid Retention Depth (FRD); from there down, porosity increases in abnormal way and pore pressure changes from a normal to an abnormal pattern. For the same well, FRD must be the same using any well log to identify it (figure 8). Swarbrick et al. (2002) underline the fact that the beginning of an abnormal pore pressure is controlled by the loading rate, the evolution of porosity and permeability of sediments during burial. The FRD is shallower in sedimentary rocks with low permability and high compressibility, and deeper in highly permeable and -low compressible rocks. In addition, for the same sediment, the FRD is shallower for high sedimentation rates and deeper for slow sedimentation rates.

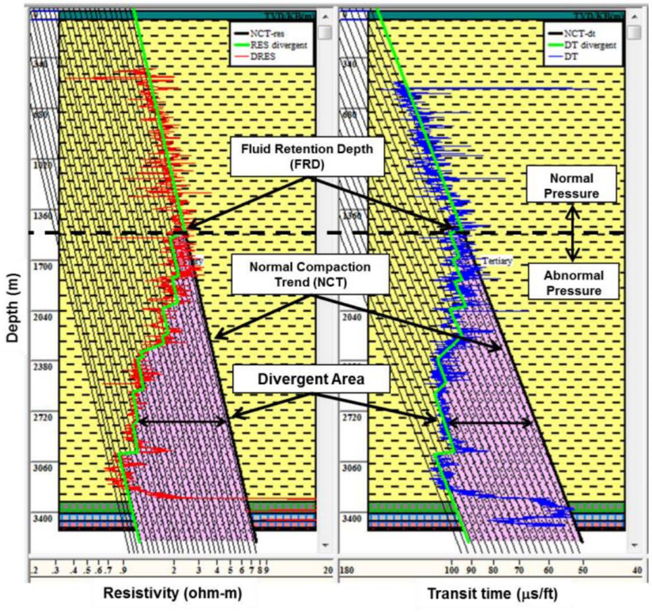

Figure 8—Identification of FRD for the same well using different well logs.

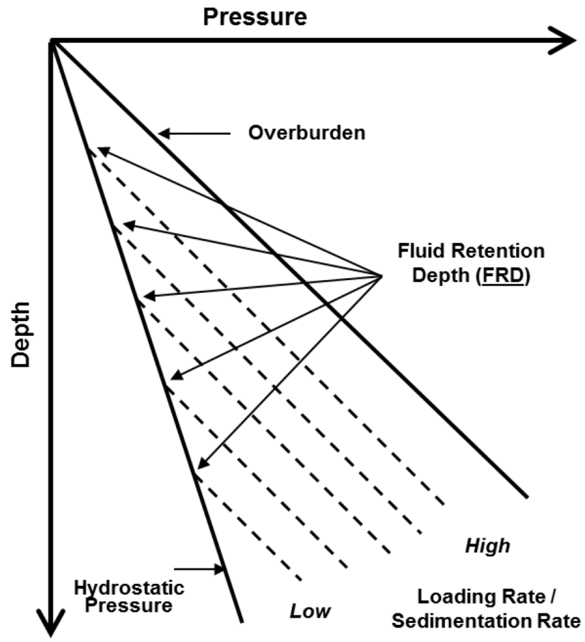

Figure 9—Behavior of FRD with loading/sedimentation rate (Modified from Swarbrick et al. 2002).

Divergent Area Methodology

The methodology is based on normal compaction of sediments trend and the way that it diverges when normal compaction is interrupted. The methodology states that if the overburden increases with depth and there is compaction disequilibrium at certain depth, the pore pressure must also increase starting in that depth. Terzaghi and Peck (1948) postulate that the overburden stress is shared by both, the fluids into the rock pores and the contact among grains; the intergranular contact stress is called effective stress (figure 10). In addition, they propose that if the pore fluid expulsion is interrupted, pore pressure increases because overburden stress increases. Hence, divergent lines and Terzaghi's model can be used to calculate pore pressure due to compaction disequilibrium as it increases when the overburden does (figure 11), as follows:

$$S = P_p + \sigma \tag{5}$$

$$\sigma = \mathrm{S} - P_p \tag{6}$$

$$\sigma_{an} = \sigma_n x DIV \tag{7}$$

$$\mathrm{DIV} = \left(\frac{\phi_n}{\phi_{an}}\right) \tag{8}$$

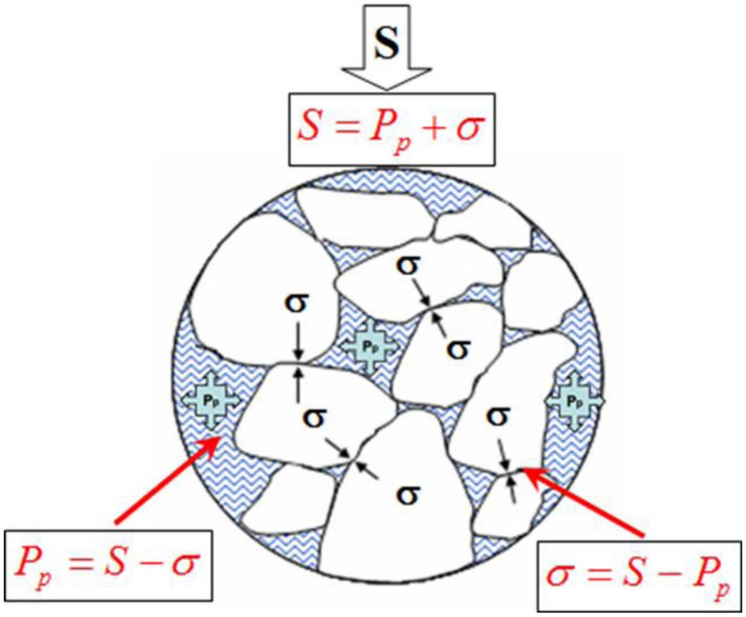

Figure 10—Illustration of Terzaghi's Model of overburden stress distribution in rock-grains and fluid.

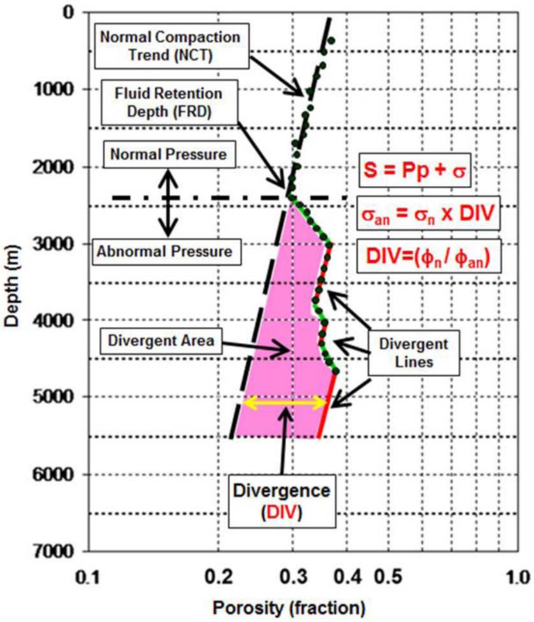

Figure 11—Divergent area coupled to Terzaghi's model.

Where:
S = Overburden stress
P_p = Pore pressure
σ = Effective stress
ϕ_n = Porosity from normal compaction trend
ϕ_{an} = Porosity from divergent lines
σ_n = Normal effective stress = $(S-Pp_n)$
σ_{an} = Abnormal effective stress = $(S-Pp_{an})$
Pp_{an} = Abnormal pore pressure
Pp_n = Normal pore pressure

DIV = Divergences

Figures 12(a), 12(b), 12(c) and 12(d) schematize the setting of a divergent area following the next procedure:

a. Plot the porosity indicator (well log) against depth and define both the NCT and FRD.
b. Draw lines parallel to NCT until well log is cover.
c. On the well log, define the transitional and parallel lines (divergences) according with its behavior, as illustrated on figure 12(c).
d. Define the divergent area and its divergent lines as shown on figure 12(d).

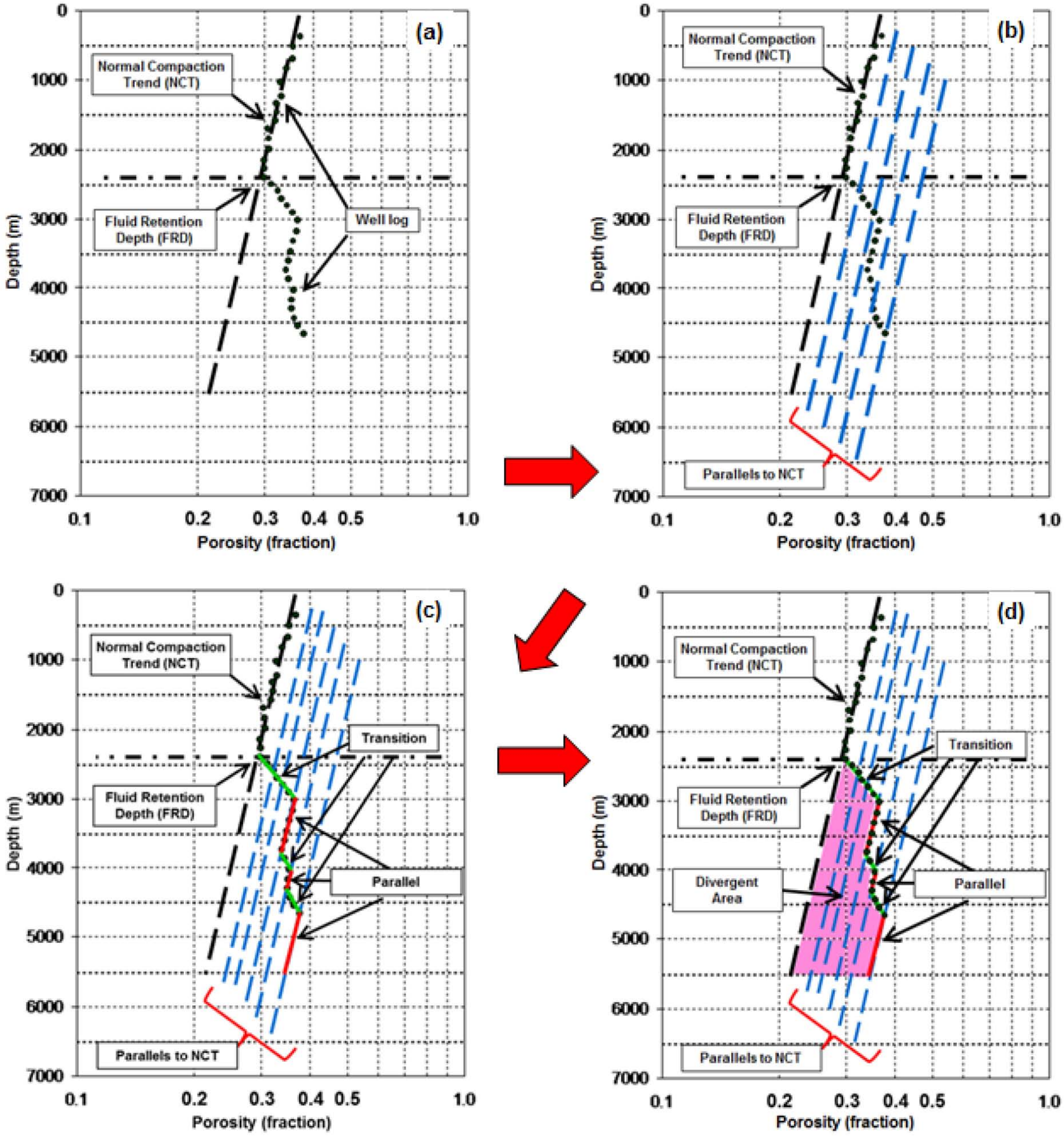

Figure 12—Steps to apply the Methodology of divergent area.

The methodology of divergent area can be applied to the reservoir rocks that do not follow in all the compaction theory of shales. Green et al. (2016) argue that one of the reasons that traditional prediction of pore pressure fails in carbonates is because the loss of porosity is not only controlled by effective stress but also by a variety of physical parameters such as depositional conditions, dissolution and diagenetic fabric history; the same occurs for sands according with Mouchet and Mitchell (1989). Figure 13 shows an illustration of underprediction of pore pressure due to porosity affected by other parameters different to compaction (modified from Green et al. 2016).

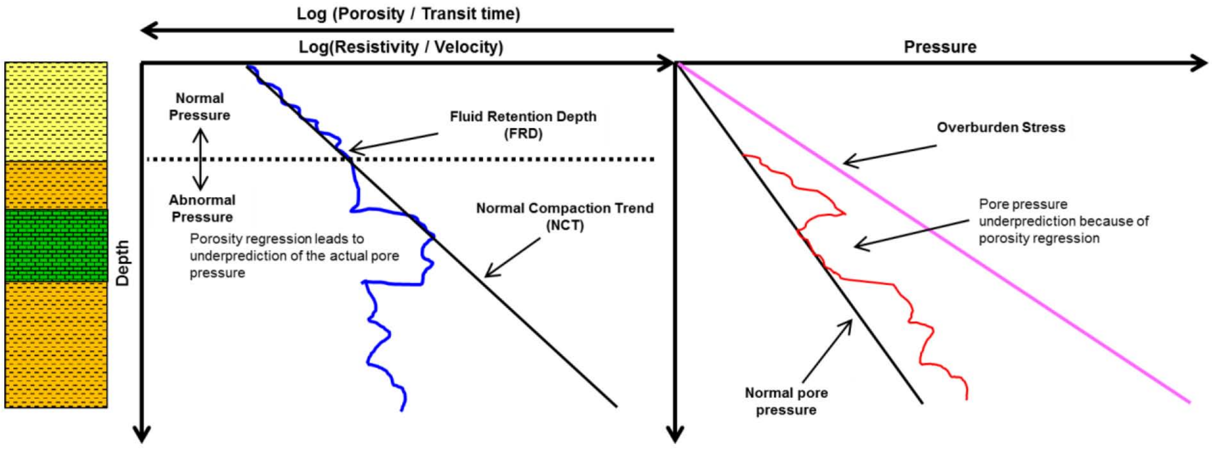

Figure 13—Underprediction of pore pressure due to porosity affected by other parameters different to compaction (modified from Green et al. 2016).

Shaker (2002) postulates that pore pressure in shales and in reservoir rocks (carbonates or sands) progresses in a cascade fashion to create a pressure envelope. Here, pore pressure in reservoir rocks follows the hydrostatic gradient while in shales it progresses expontentially from top to bottom. Figure 14 shows the pressure envelope following Shaker's postulate (2002). Hence, considering the pressure envelope illustrated in figure 14, the methodology of divergences may be used to infer pore pressure in reservoir rocks like carbonates or sands. The divergence application consist in to identify transitional behaviors of the porosity indicators (shale) and those that are parallel to normal compaction trend (reservoir rock) and then, build a divergent area as show in figure 15.

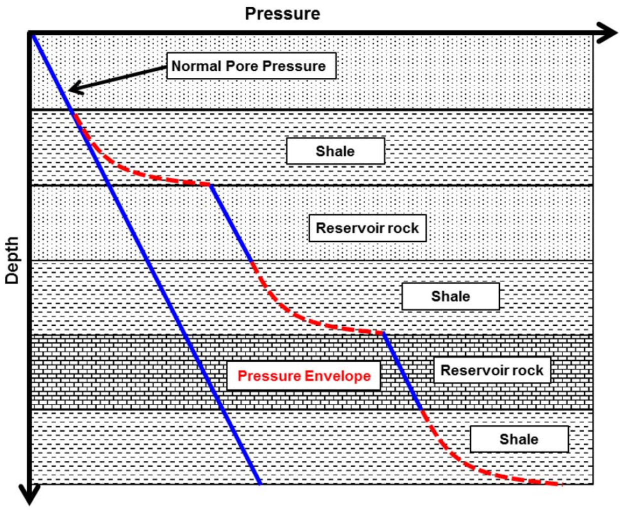

Figure 14—Illustration of pressure envelope (modified from Shaker 2002).

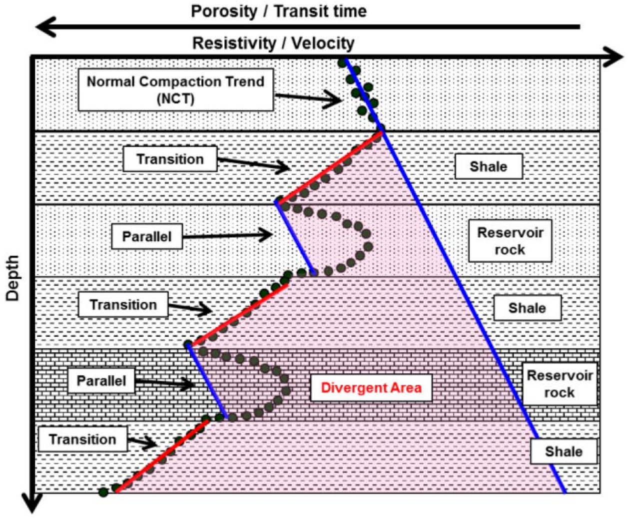

Figure 15—Divergent area to infer pore pressure in reservoir rocks.

Once the divergent area is defined, the pore pressure calculation can be done using a pore pressure model based on normal compaction theory, such as Eaton's, along with the use of either well logs and/or interval velocity from seismic.

Overburden Stress Correction

Overburden stress at a given depth is the stress exerted by the weight of the overlying sediments; therefore, it may be determined by means of bulk density of the sediments by the following equation:

$$S = \int_0^Z \rho_r g dZ = \sum_{i=1}^{n} \rho_{ri} g \left[Z_i - Z_{i-1} \right] \tag{9}$$

Where:
S = Overburden stress
ρ_{ri} = Bulk density due to mechanical compaction at depth i
g = Acceleration of gravity
Z_i = Depth i
Z_{i-1} = Depth before i

The bulk density profile of a rock formation is acquired by well density log, however, the density log may be affected by overpressures, gas content, borehole washouts and high mud filtrates among others. These effects influence the density log readings and consequently the overburden stress calculations; furthermore, the lack of density log readings in the first drilling stages also affects the overburden stress calculations. Nevertheless, the most important issue in overburden stress calculation is that it must be determined exclusively using the rock bulk density due to normal compaction of sediments. Eaton (1969, 1972) discusses the integration of bulk density graphs built from several well logs taken in normally compacted formations in the Gulf Coast and Santa Barbara Channel. From those graphs, he build his overburden stress nomogram for each location discussed. Mouchet and Mitchell (1989) remark that most clays may be normally compacted but the loss of porosity in carbonates and sands depends also on many other parameters, such as diagenetic effects, sorting, original composition and others. Figure 16 shows the bulk density nomogram built by Eaton (1969) from several normally compacted wells in the Gulf Coast; Figure 17 presents a density log influenced by overpressures, borehole conditions and other parameters different to normal compaction of sediments which the end, impact the overburden calculations.

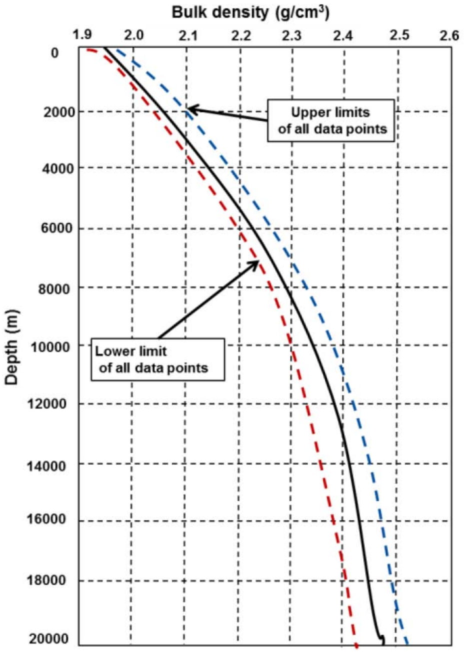

Figure 16—Bulk density from normally compacted formations in the Gulf Coast (Modified from Eaton 1969).

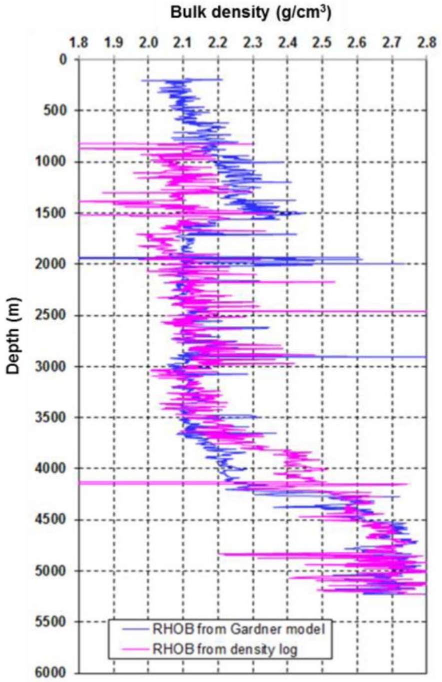

Figure 17—Bulk density from Mexican well.

To avoid the "*environmental*" effects in density log readings, a modification to equation (9) is proposed as follows:

$$S = \sum_{i=1}^{n} \left(\rho_o + kZ^c \right) \cdot g \cdot \left[Z_i - Z_{i-1} \right] \tag{10}$$

Where:
S = Overburden stress

ρ_0 = Bulk density at surface
c = Normal compaction behavior index (varies from 0.3 to 0.6)
k = Declination parameter (0.01)
g = Acceleratioin of gravity
Z_i = Depth i
Z_{i-1} = Depth before i

Equation (10) considers that bulk density vary normally with compaction of the sediments as depth increases. This correction avoids the "*environmental*" effects of density log readings as observed in two Mexican wells presented in figure 18.

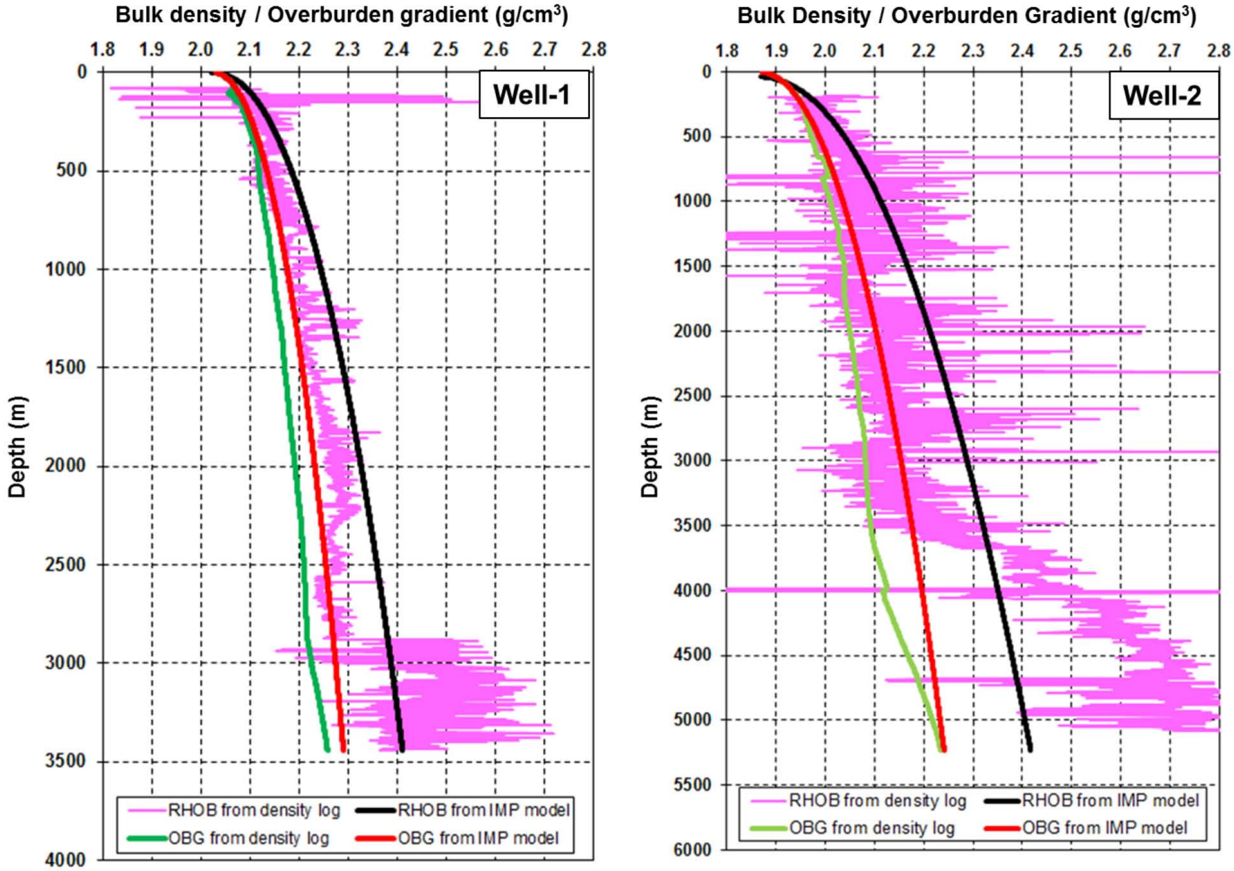

Figure 18—Overburden influenced by the "environmental" effects of density log readings in two Mexican wells.

Fitting of Pore Pressure Model

The first recommendation that different authors make of the use of their pore-pressure models is that they have to be adjusted to the conditions of each particular geological basin (Hottmann and Johnson 1965; Eaton 1975; Bowers 1995). For instance, studies of pore pressure, done in offshore wells at the Mexican Gulf Coast, show that the original Eaton's model "overestimate" pore pressure when compared to measured values (Velazquez-Cruz et al. 2008). To regionalize Eaton's pore-pressure model, the convergence analysis approach was applied, as it was explained before; however, alpha exponent (**α**) from Eaton equation was a great unknow until it was evaluated with the resistivity and sonic travel time data from several wells drilled at Mexican Gulf Coast. The results revealed that the alpha exponent is smaller than its original value for both logs; results are showed in table 1.

Table 1—Values of alpha exponent for wells drilled at Mexican Gulf Coast.

Source	Alpha exponent for resistivity	Alpha exponent for sonic transit time
(Eaton 1975)	1.2	3.0
This Work	0.12	0.30

Figure 19 shows a pore pressure analysis in a Mexican offshore well using sonic transit time and Eaton's equation with alpha exponent equal to three. Figure 20 presents the same well with alpha exponent equal to 0.3.

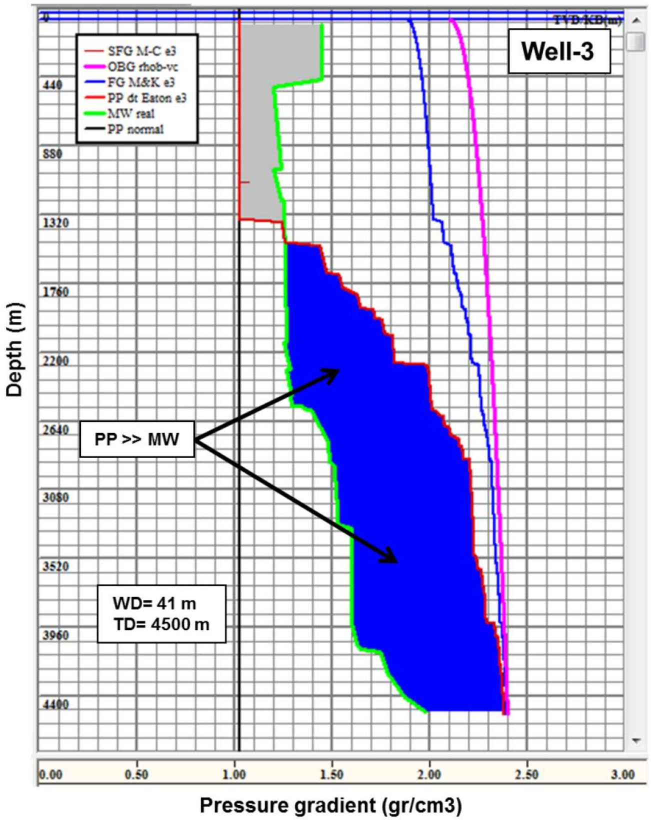

Figure 19—Pore pressure of Mexican offshore well 3 with Eaton's exponent alpha equal to three.

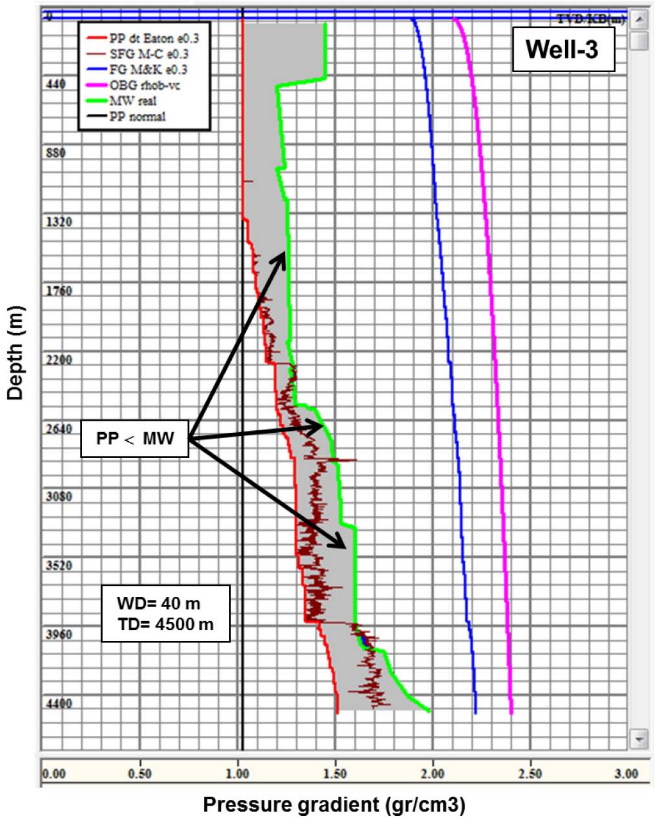

Figure 20—Pore pressure of Mexican offshore well 3 with Eaton's exponent alpha equal to 0.30.

Case Analysis

The convergence analysis of pore pressure was applied to an onshore well in Mexico as it shown in figure 21. Track No. 1 displays the gamma ray log without shale points pick, which are not required when the divergent area is used. Track No. 2 present the analysis of "divergent lines" to identify transitional behaviors of the porosity indicators (at the shale) and those that are parallel to normal compaction trend (at the reservoir rock) which, when coupled to the normal compaction trend, help to build the divergent area. In addition, track 2 exhibits a reservoir rock portion with a porosity regression that without use of the divergent area, may lead to an underprediction of the pore pressure as illustrated in figure 13. Furthermore, the methodology of divergences replaces the shale points interpolation for the analysis of the compaction disequilibrium phenomena directly in the well log. Track No. 3 expose the pore pressure analysis of the well, here, it can be observed how the pore pressure increases steadily and uniformly, properly describing the effect of the overburden pressure.

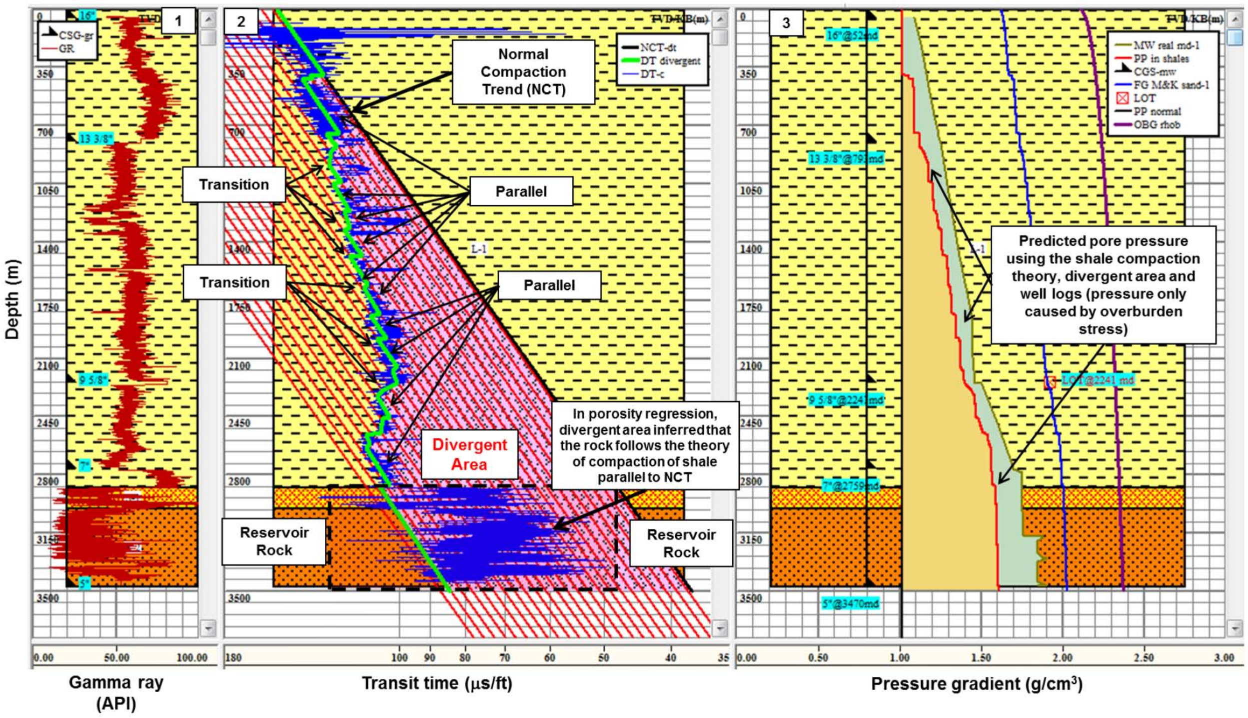

Figure 21—21. Pore pressure analysis using the shale compaction theory, divergent area and well logs in Mexican onshore well.

Conclusions

- The NCT represents the porosity loss with depth so that any well would have a unique NCT.
- The NCT is the keystone of pore pressure analysis and breaking the NCT into several segments for calibration purposes must be avoided.
- As burial depth increase, porosity reduces until a depth known as Fluid Retention Depth (FRD), which is unique, so that for the same well, the FRD must be the same regardless of the well log used to identify it.
- The methodology of divergences allows developing a pore pressure prognosis based on the behavior of well logs due to normal compaction of sediments, avoiding the use of lithological logs and the selection of shale points.
- The methodology of divergences may be applied to the reservoir rocks that do not follow in all the compaction theory of shales.
- When the divergent area is defined, the pore pressure calculation could be done using both, a pore pressure model based on normal compaction theory and well logs or interval velocity from seismic.
- To avoid misdeterminations of overburden stress, the rock bulk density due exclusively to normal compaction of sediments must be used instead straight density log readings.
- The models to predict pore pressure must be adjusted to local geological conditions.
- The alpha exponent from Eaton's equation was found smaller for the Mexican Gulf Coast than that for the Louisiana Gulf Coast.
- The methodology of divergences is properly coupled to the theory of compaction and to pore pressure analysis based on well logs and seismic, i.e., if the overburden stress increases with depth and there is compaction disequilibrium, the pore pressure must be increased with depth.

Acknowledgments

The authors would like to thank Instituto Mexicano del Petróleo for the support to develop this paper.

Nomenclature

c = *Normal compaction behavior index*
CSG = *Casing depth*
DIV = *Divergences*
DRES = *Deep Resistivity*
DT = *Sonic Transit Time*
FG = *Fracture gradient*
FRD = *Fluid Retention Depth*
GR = *Gamma Ray*
k = *Declination parameter*
LOT = *Leak Off Test*
MDT = *Modular formation Dynamic Tester*
MW = *Mud Weight*
NCT = *Normal Compaction Trend*
NPT = *Non-Productive Time*
OBG = *Overburden gradient*
P_p = *Pore pressure*
P_{pan} = *Abnormal pore pressure*
P_{pn} = *Normal pore pressure*
RHOB = *Bulk density*
R_n = *Normal compaction trend for resistivity*
R_o = *Resistivity at surface*
S = *Overburden stress*
SFG = *Shear Failure Gradient*
SHPT = *SHale PoinT*
TD = *Total Depth*
V_n = *Normal compaction trend for interval velocity*
V_o = *Interval velocity at surface*
WD = *Water Depth*
Z = *Depth*
Δt_n = *Normal compaction trend for sonic transit time*
Δt_o = *Sonic transit time at surface*
ϕ_{an} = *Porosity from divergent lines*
ϕ_n = *Normal compaction trend for porosity*
ϕ_o = *Porosity at surface*
ρ_0 = *Bulk density at surface*
σ = *Effective stress*
σ_{an} = *Abnormal effective stress*
σ_n = *Normal effective stress*

References

1. Athy, L. F. (1930). Density, Porosity, and Compaction of Sedimentary Rocks. *AAPG Bulletin*, v. **14**, p. 1–23, 1930.
2. Bowers, G. L. (1995). *Pore Pressure Estimation from Velocity Data: Accounting for Overpressure Mechanisms besides Undercompaction*. Society of Petroleum Engineers. http://doi:10.2118/27488-PA

3. Bowers, G.L. (2002). Detecting High Overpressure. *The Leading Edge*, v. **21**, no. 2, p. 174–177.
4. Correa, O. (2016). Modelo que Describe la Compactación Normal para la Cuenca de Burgos y su Aplicación a la Presión de Poro. Tesis de Maestría en Ingeniería en Exploración y Explotación en Recursos Naturales, Universidad Nacional Autónoma de México, Ciudad de México.
5. Eaton, B. A. (1969). *Fracture Gradient Prediction and Its Application in Oilfield Operations*. Society of Petroleum Engineers. http://doi:10.2118/2163-PA.
6. Eaton, B. A. (1972, August 1). *The Effect of Overburden Stress on Geopressure Prediction from Well Logs*. Society of Petroleum Engineers. http://doi:10.2118/3719-PA.
7. Eaton, B. A. (1975). *The Equation for Geopressure Prediction from Well Logs*. Society of Petroleum Engineers. http://doi:10.2118/5544-MS.
8. Green, S., O'Connor, S. A., and Edward, A. P. (2016). Predicting Pore Pressure in Carbonates: A Review. *Search and Discovery Article #41830* (2016).
9. Hamid, O., Khan, K., Rahim, Z., Omair, A., Ahmed, S., & Ahmed, M. (2016, November 14). Reducing Drilling Operational Risk and Non-Productive Time Using Real-Time Geomechanics Surveillance. International Petroleum Technology Conference. http://doi:10.2523/IPTC-18793-MS.
10. Hoskin, E. and O'Connor, S. A. (2016). The consequences of ignoring rock properties when predicting pore pressure from seismic and sonic velocity. *First break*, volume **34**, October 2016.
11. Hottmann, C. E., & Johnson, R. K. (1965). *Estimation of Formation Pressures from Log-Derived Shale Properties*. Society of Petroleum Engineers. http://doi:10.2118/1110-PA.
12. López-Solís, V., Velázquez-Cruz, D., Jardinez-Tena, A., & Castañeda, G. E. (2006). Normal Resistivity Trends for Geopressure Analysis in Mexican Offshore Wells. Offshore Technology Conference. http://doi:10.4043/18192-MS.
13. Mouchet, J. P., and Mitchell, A. (1989). *Abnormal Pressure While Drilling*. Elf-Aquitaine, Boussens, France, Technical Manual No. 2, 255 p.
14. Ong, S. H., Power, W. L., Sitio, A., & Tanjung, E. (2015). *Geomechanics Improves Drilling Operations and Reduces Non-Productive Times (NPT) in Kilo Field, Offshore Northwest Java*. Society of Petroleum Engineers. http://doi:10.2118/176445-MS.
15. Pennebaker, E. S. (1968). *An Engineering Interpretation of Seismic Data*. Society of Petroleum Engineers. http://doi:10.2118/2165-MS.
16. Shaker, S. (2002). Causes of Disparity between Predicted and Measured Pore Pressure. *The Leading Edge*, August 2002, Vol. **21**, No.8.
17. Shaker, S. (2007a). Calibration of Geopressure Predictions using Normal Compaction Trend: Perception and Pitfall. *Canadian Society of Exploration Geophysicists, Recorder*, January 2007.
18. Shaker, S. (2007b). The Precision Of Normal Compaction Trend Delineation Is The Keystone Of Predicting Pore Pressure. AADE (American Association of Drilling Engineers), Annual Convention, April 2007, Houston, Texas, Paper #51.
19. Swarbrick, R. E. and Osborne, M. J. (1998). Mechanisms that Generate Abnormal Pressures: An Overview. In Law, B. E.; Ulmischek, G. F.; and Slavin, V. I., eds, *Abnormal Pressures in Hydrocarbon Environments*, AAPG Memoir **70**, p. 13 – 34.
20. Swarbrick, R.E., Osborne, M.J., and Yardley, G.S. (2002). Comparisons of overpressure magnitude resulting from the main generating mechanisms, chapter 1. In Huffman, A., and Bowers, G., editors, *Pressure regimes in sedimentary basins and their prediction*; AAPG Memoir No. 76, p. 1–12.
21. Terzaghi, K. and Peck, R. B. (1948). *Soil Mechanics in Engineering Practice*. John Wiley and Sons.

22. Velázquez-Cruz, D.; Lopez-Solis, V.M.; Díaz-Viera, M.A. (2008). Avances en la Determinación de Presiones Anormales en la Costa Mexicana del Golfo. *Revista Ingeniería Petrolera, Diciembre del 2008*, Vol. **XLVIII**, No.12.
23. York, P. L., Prichard, D. M., Dodson, J. K., Dodson, T., Rosenberg, S. M., Gala, D., & Utama, B. (2009). Eliminating Non-Productive Time Associated with Drilling through Trouble Zones. Offshore Technology Conference. http://doi:10.4043/20220-MS.